

Supplementary Material

	<u>ASD (n=15)</u> Mean (SD), Range	<u>TD (n=20)</u> Mean (SD), Range	p-value
Age	11.4 (3.7), 8-18	11.9 (2.8), 8-18	0.6
SCQ Lifetime	21.6 (4.5), 16-28	4.4 (3.5), 0-13	0.0004
SCQ Current	17.1 (5.1), 7-25	4.6 (2.9), 1-11	0.000008
ADOS Combined	11.5 (3.5), 7-19	2.2 (1.8), 0-5	0.000000002
ADOS Soc	7.8 (2.5), 5-13	1.5 (1.3), 0-4	0.00000002
ADOS Comm	3.7 (1.2), 2-6	.7 (.7), 0-2	0.00000003
Verbal IQ	110 (15.8), 83-141	110.6 (15.6), 80-141	0.9
Nonverbal IQ	101.5 (19.2), 73-144	110.4 (17.0), 77-140	0.2
Touch Score	55.7 (12.5), 34-74	81.4 (8.1), 60-90	0.0000005
Multisensory Processing Score	22 (4.94) 16 - 31	30.4 (4.92) 15 - 35	0.00004

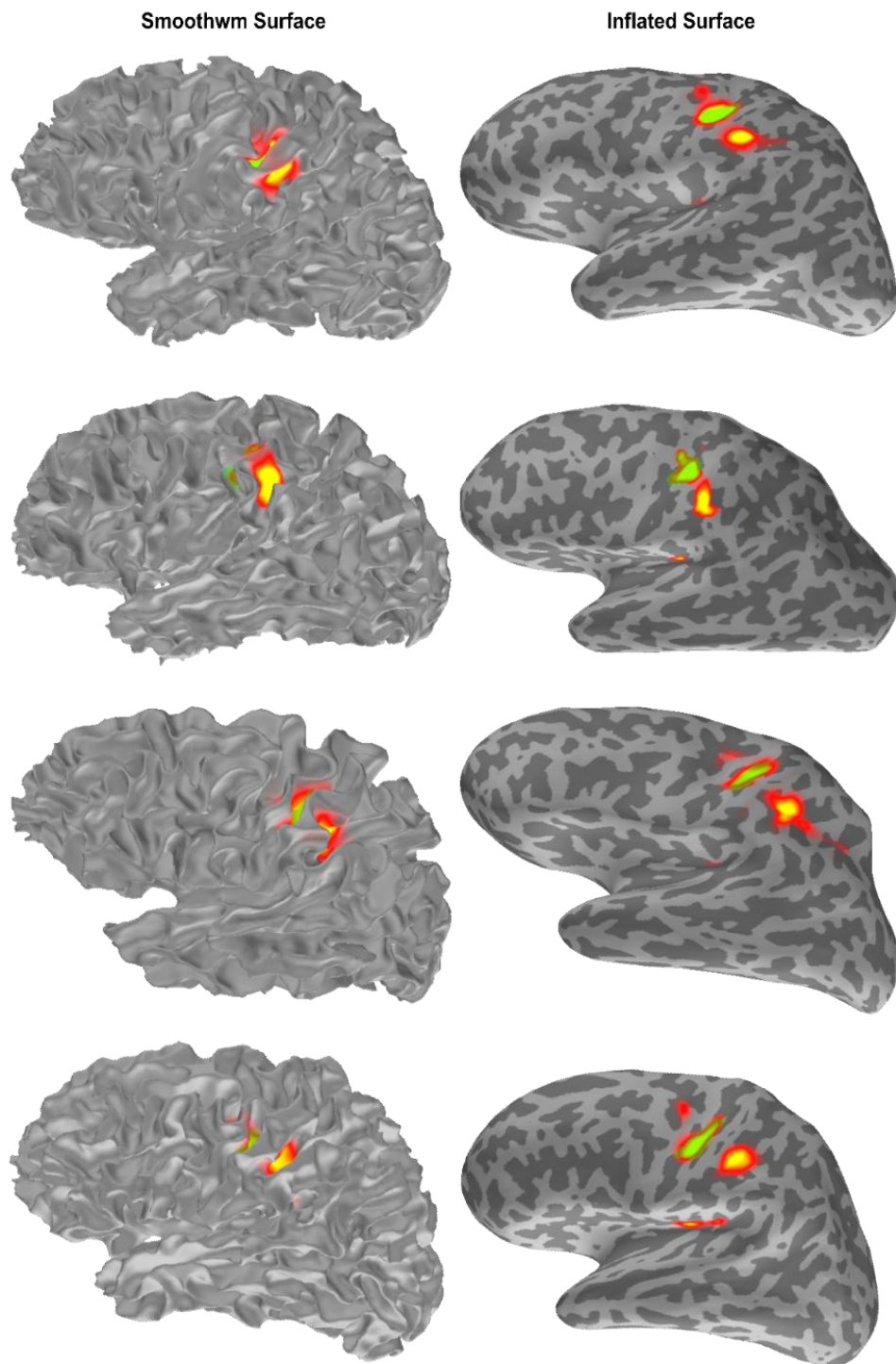
Table 1: Participants in Vibrotactile experimental paradigm. As expected, only ADOS/SCQ scores and sensory processing scores were significantly different between the groups.

	<u>ASD (n=12)</u> Mean (SD), Range	<u>TD (n=12)</u> Mean (SD), Range	p-value
Age	12.2 (3.6), 8-18	12.08 (2.81), 8-16	0.9
SCQ Lifetime	21.6 (4.5), 16-28	4 (2.6), 0-7	0.0000003
SCQ Current	16.1 (5.1), 7-21	5.2 (1.9), 3-8	0.0005
ADOS Combined	10.7 (2.9), 7-16	1.4 (1.8), 0-4	0.0000009
ADOS Soc	7.2 (2.1), 5-11	1.0 (1.3), 0-3	0.000002
ADOS Comm	3.5 (1.1), 2-5	.4 (.5), 0-1	0.000002
Verbal IQ	109.6 (17.6), 83-141	110.0 (15.84), 80-141	0.9
Nonverbal IQ	98.1 (16.2), 73-136	108.0 (18.1), 77-140	0.2
Touch Score	56.7 (12.6), 34-74	83.3 (7.6), 67-90	0.000003
Multisensory Processing Score	22.5 (5.2) 16 - 31	31.6 (3.6) 26 - 35	0.00006

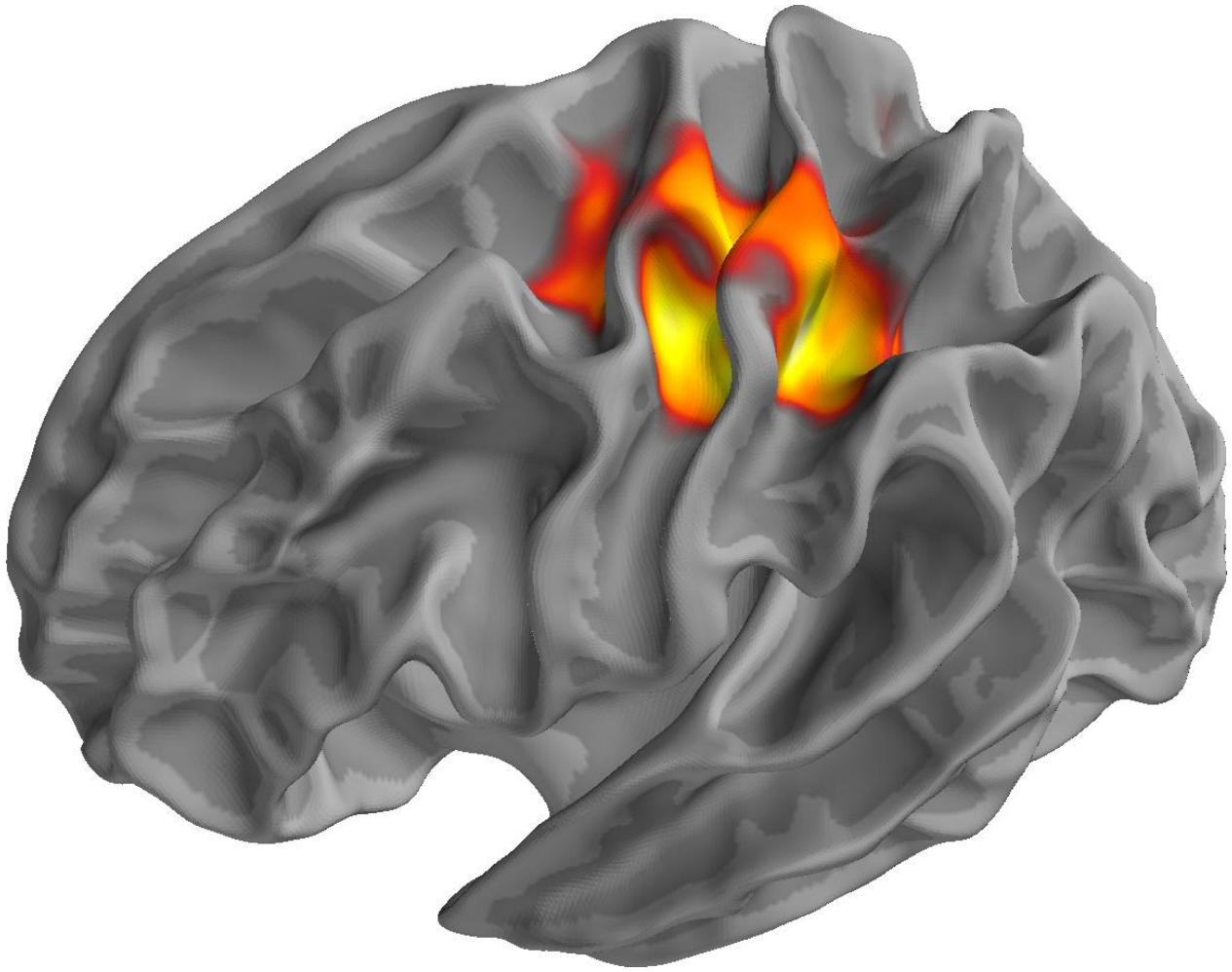
Table 2: Participants in the resting state experimental paradigm, a subset of the participants listed in table S1. Again, as expected, only ADOS/SCQ scores and sensory processing scores were significantly different between the groups. Note that the participants here are the subset of the participants in Kitzbichler et al, 2014 that have also completed the vibrotactile experiment.

Subject	S1			S2		
1	-51.8423	-24.3028	47.136	-41.2253	-20.3063	18.21319
2	-54.4926	-18.553	48.27227	-33.8452	-30.1263	21.09068
4	-44.8687	-21.5806	55.68291	-35.4878	-33.9413	19.85211
4	-49.4309	-20.308	44.48448	-40.2792	-26.194	22.30419
5	-33.0634	-17.1034	40.40929	-39.8095	-24.5961	21.14938
6	-39.1854	-27.8992	51.96064	-34.139	-34.0127	18.09552
7	-51.06	-17.719	51.44418	-37.4818	-25.3549	21.18082
8	-37.2633	-26.6151	46.07749	-43.5647	-27.3748	22.2706
9	-34.4264	-23.2237	46.84764	-40.8934	-11.3442	18.89238
10	-52.9129	-17.9369	50.02635	-33.4114	-22.4885	19.1855
11	-32.1146	-30.518	51.9427	-34.0039	-12.7758	16.657
12	-36.0155	-21.1847	36.19466	-35.5662	-27.8061	21.56158
13	-33.0962	-22.0185	46.20281	-34.7287	-7.28011	10.50186
14	-33.5535	-20.2713	48.6585	-39.7338	-64.0654	31.91693
15	-54.683	-19.9152	49.70838	-35.9799	-23.0517	20.70603
16	-57.0836	-17.7983	39.47779	-31.1936	-27.7909	17.05668
17	-33.4135	-15.8436	44.95144	-43.6162	-15.2286	19.82064
18	-38.4679	-13.5111	41.66974	-38.4924	-20.1492	20.64
19	-41.4234	-20.9619	34.35546	-39.3513	-22.8	19.69173
20	-34.3226	-28.4203	47.42018	-37.2808	-13.1733	20.09368
21	-41.2076	-22.3147	47.91122	-36.5565	-16.305	20.5304
22	-43.3686	-21.0798	50.2832	-36.2073	-29.4531	22.12241
23	-33.0934	-21.716	41.62169	-35.487	-6.66577	9.216394
24	-45.5715	-21.572	41.71088	-43.4415	-21.6584	19.05854
25	-35.6509	-16.5656	36.95115	-34.1571	-19.6048	13.81518
26	-41.1136	-13.5976	30.27096	-43.6015	-0.36336	13.45616
27	-39.1829	-23.2187	45.79089	-31.311	-30.0482	17.26505
28	-32.2881	-19.5539	40.59275	-35.9596	-12.8557	19.263
29	-56.5795	-18.7005	43.04819	-32.747	-22.6748	15.21184
30	-34.9402	-14.4469	47.6309	-42.5736	-11.7357	18.99627
30	-51.6482	-18.647	53.2713	-31.3935	-27.3711	9.275659
32	-37.3812	-20.7501	34.86623	-45.6753	-10.4306	16.21627
33	-51.1082	-20.9283	53.71957	-31.4234	-25.3451	14.65858
34	-37.4339	-13.0268	47.7788	-37.5485	-33.2111	20.73342
35	-41.4934	-16.7316	31.03368	-37.936	-26.977	22.12511

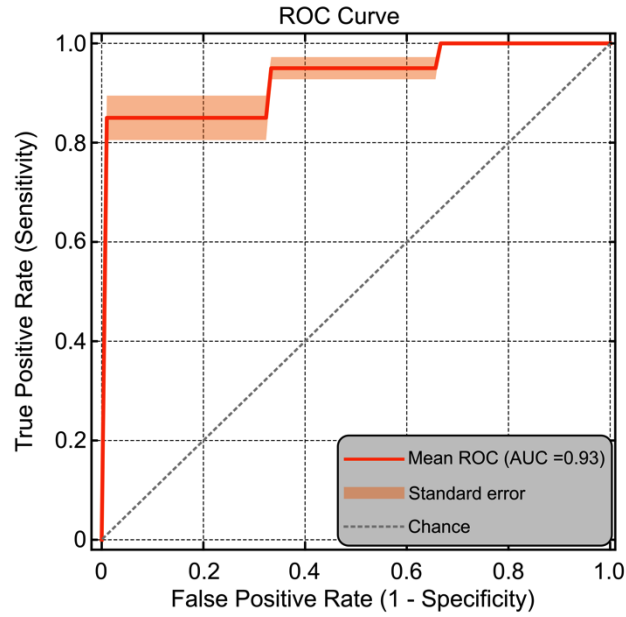
Supplementary Table 3: MNI Co-ordinates of each participant for S1 and S2. The computations were carried out on the surface, using FreeSurfer RAS coordinates, and then transformed to volume coordinates.



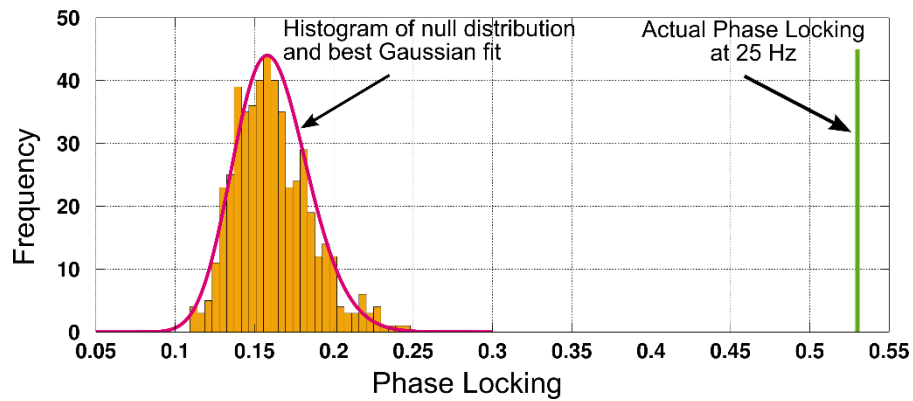
Supplementary Figure 1: Inter-subject variability in S1 location, shown on the smooth white matter surface (left) and inflated brain (right). Each row represents one participant, chosen at random. While on the inflated brain areas might seem distant and disjoint, it is obvious from the left column that these areas are in fact adjacent in the brain, and are just different sides of the same sulci. The two top participants are from the TD group, and two bottom ones are from the ASD group. Variability in S1/S2 localization was similar across both groups.



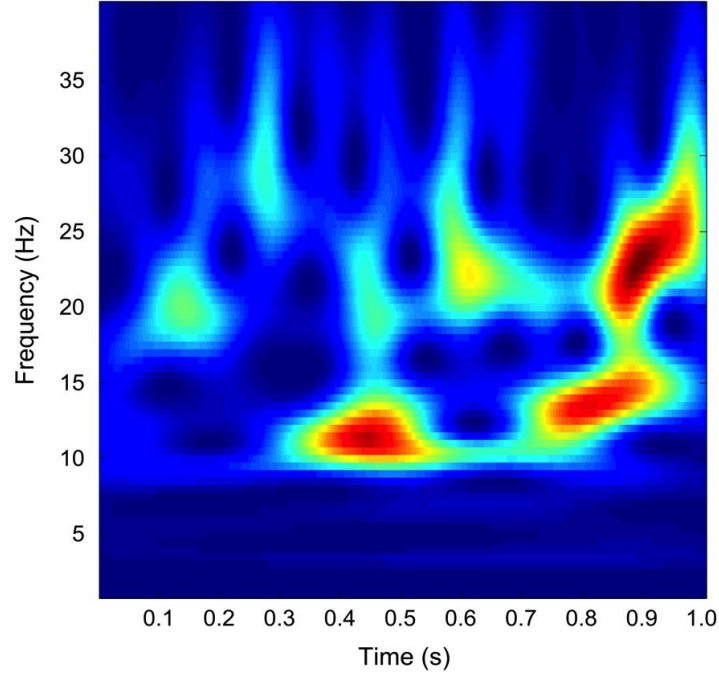
Supplementary Figure 2: Figure 4B (top) visualized on the folded cortex, on the uninflated brain. The widespread distribution on the inflated cortex is much more compact in the actual folded cortical surface, illustrating that most of the extent is likely due to the point spread of the MNE.



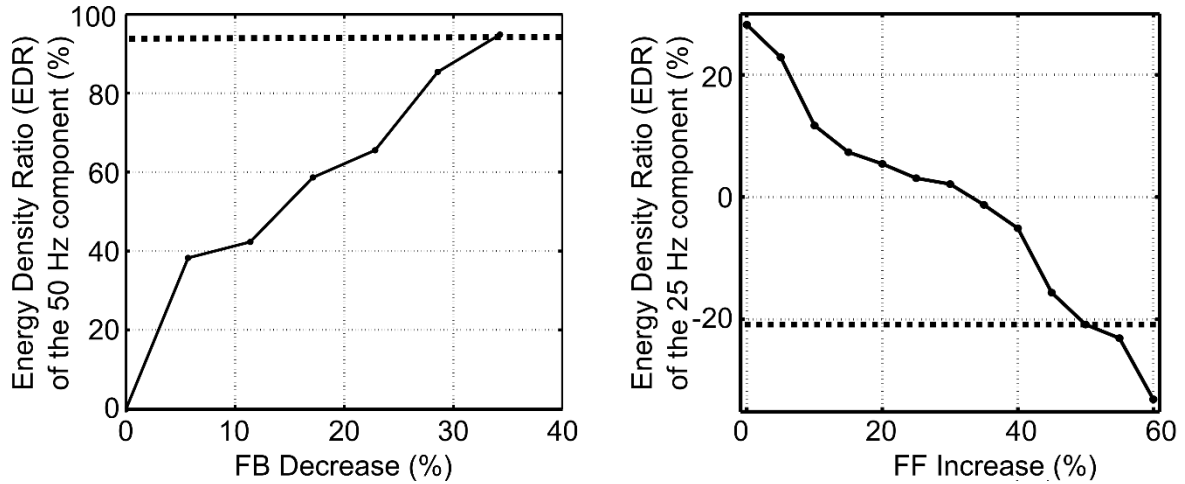
Supplementary Figure 3: ROC curve for figure 8D.



Supplementary Figure 4: Calculating Z-PL. The null distribution was computed as described in the experimental procedures section, and is shown here in orange. For each PL value in the data, we then compute Z-PL using the mean and variance of the Gaussian distribution giving the best fit to the empirical null distribution.



Supplementary Figure 5: Model output for mu-alpha and mu-beta (Jones et al., 2009). The model parameters used here are the same as those used in the original publication.



Supplementary Figure 6: MEG data-driven estimation of the simulated feedforward (FF) and feedback (FB) ratios for replicating the ASD group results. *Left panel* – The Energy Density Ratio (EDR) change of the 50 Hz component between TD and ASD was measured to be 94% in the MEG data. For the simulated TD signal, the conductance of the neural model was 40 pS and the FF and FB conductance gains were 1 and 3.5, respectively. Simulations showed that in order to obtain a 94% change in the EDR_{50} , the strength of the model's FB gain needed to decrease by 32%. *Right panel* – After fixing the model's FB gain to 2.4, we adjusted the FF gain to match the MEG measured EDR value for the 25 Hz component between TD and ASD, which was -21%. To obtain a -21% EDR_{25} in the simulations, the FF gain needed to increase by 50%. The EDR_{50} did not change with FF increase.

A

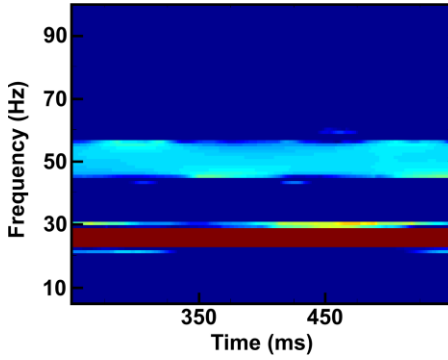
$$S = \sum_{n=1}^{80} [\sin(2\pi 25t + \phi_n^1) + \sin(2\pi 50t + \phi_n^2) + \zeta_n]$$

$$t \in [250\text{ms}, 550\text{ms}], \phi \in (0, 15\text{ms}], \zeta \in N(0, 1)$$

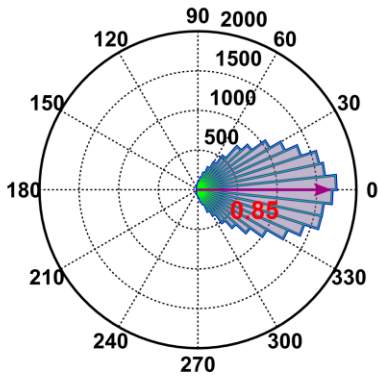
Same jitters
between 25Hz and 50Hz

$$\phi_n^1 = \phi_n^2$$

Phase locking with respect to Stimulus onset

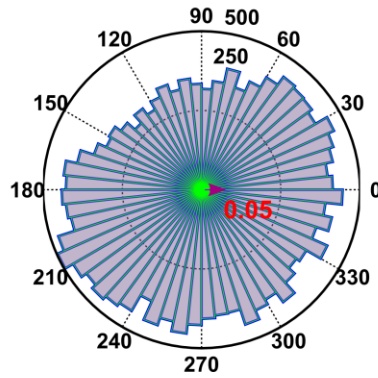
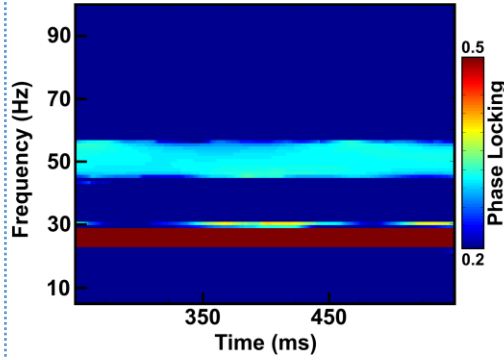


Phase locking between 25Hz and 50Hz



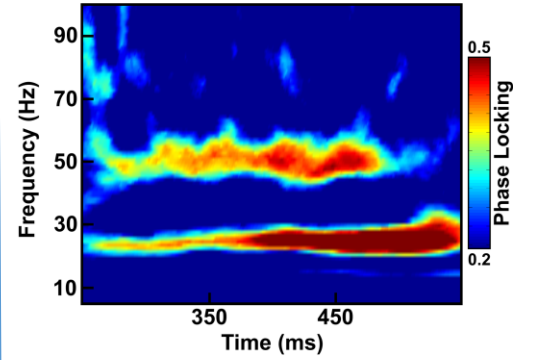
Different jitters
between 25Hz and 50Hz

$$\phi_n^1 \neq \phi_n^2$$

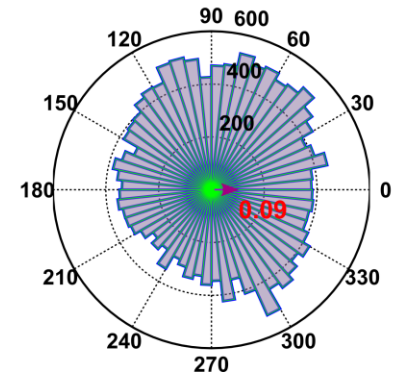
**B**

Typical TD Subject

Phase locking with respect to Stimulus onset



Phase locking between 25Hz and 50Hz



Supplementary Figure 7: No phase locking between the 25Hz and 50 Hz components of the response.

We hypothesize the two components are not phase locked due to different, and independent, jitters, resulting from the different synaptic recruitments for the two components. **(A)** Simulation study, showing an input signal S . In the first case, on the left, there is no jitter between the two components, and the phases are locked, as shown on the phase plot at the bottom. In the second case, on the right, there is a random jitter difference, and the phases across the components are random relative to one another. **(B)** Same analysis, applied to the data from a representative TD participant. The results are clearly in line with the “independent jitters” scenario presented on the right side of panel A. Note that since a very strong S/N is needed for this analysis, we carried out the computation only in the 8 TD participants with the highest 50Hz component, with similar results.